
NONLINEAR
AND QUANTUM OPTICS

Collisions of Single-Cycle and Subcycle Attosecond Light Pulses in a Nonlinear Resonant Medium

R. M. Arkhipov^{a, b, *}, M. V. Arkhipov^{a, b}, A. V. Pakhomov^b, D. O. Zhiguleva^{a, c}, and N. N. Rosanov^{b, d, e}

^a St. Petersburg State University, St. Petersburg, 199034 Russia

^b ITMO University, St. Petersburg, 197101 Russia

^c Heinrich Heine University, 40225 Düsseldorf, Germany

^d Vavilov State Optical Institute, St. Petersburg, 199053 Russia

^e Ioffe Physical Technical Institute, Russian Academy of Sciences, St. Petersburg, 194021 Russia

*e-mail: arkhipovrostislav@gmail.com

Received December 12, 2017

Abstract—By numerically solving the system of Maxwell–Bloch equations, we have examined theoretically collisions of extremely short single-cycle and unipolar subcycle pulses in a nonlinear resonant medium under conditions that the light interacts coherently with the medium. The dynamics of the electric field of structures of light-induced polarization and inversion difference has been considered in the situation in which pulses are overlapped in the medium. We show that the states of the medium (to the right and to the left of the overlap region of the pulses) may differ. In particular, we show that polarization waves with different characteristics can exist in the regions of the medium that are located on opposite sides of the overlap region of the pulses. These waves travel in different directions and have different spatial frequencies.

DOI: 10.1134/S0030400X18040045

INTRODUCTION

At present, due to the method of generation of high-order optical harmonics, it has become possible to form extremely short pulses with their duration in the attosecond range ($1 \text{ as} = 10^{-18} \text{ s}$) [1–3]. The use of these pulses gave the possibility of studying many fundamental issues related to the structure of matter. For example, it became possible to investigate and control the dynamics of wave packets in atoms, molecules, and solids [4, 5], as well as in metal and dielectric nanostructures [6], to study the dynamics of electron tunneling through potential barriers [7], to accelerate electron beams [8], etc.

The duration of extremely short pulses in a resonant medium is much shorter than the relaxation times of the polarization, T_2 , and the population difference, T_1 . Therefore, under these conditions, if the central frequency of a pulse coincides with the frequency of a resonance of the medium, manifestations of the coherent interaction of the pulse with the medium are possible. The coherent interaction manifests itself in the appearance of Rabi oscillations of the atomic polarization and the population inversion, and it can lead, e.g., to the phenomenon of self-induced transparency [9]. In this case, the 2π pulse of self-induced transparency propagates in the medium without losses. The interaction of extremely short pulses with various media was thoroughly studied theoretic-

ally and experimentally under conditions if the spectrum of pulses is far from the resonant frequency of the medium, and the manifestation of coherent effects in the form of Rabi oscillations is impossible (see reviews [10–13] and references therein). The coherent propagation of pulses and the effect of self-induced transparency were examined experimentally only for long pulses in different media (gases, vapors of alkali metals) [14–16]. Recently, it has been possible to observe the effect of self-induced transparency and the appearance of Rabi oscillations in semiconductor structures on quantum dots [17–20]. Recent experiments should be noted in which Rabi oscillations were observed [21–25], as well as Ramsey fringes [26] in quantum dots interacting with femtosecond-long pulses at room temperature.

At the same time, there are many works in which the coherent propagation of extremely short pulses in a resonantly absorbing medium has been studied theoretically [27–53]. However, investigations performed in these works were mainly focused on studying aspects of the coherent propagation of extremely short pulses, such as the verification of the satisfiability of the McCall–Hahn area theorem [39–41], checking the validity of the approximation of slowly varying amplitudes and of the rotating-wave approximation [42–45], studying soliton propagation regimes and the generation of attosecond pulses [27, 32–38], induc-

tion and ultrafast control of light-induced structures using single-cycle [46, 47, 50] and subcycle [48, 49, 51] pulses.

These investigations were done mainly for the case of bipolar pulses, for which the electric-field strength changes its sign with time and the electric area of the pulse, which is defined as the integral of the electric-field-strength vector at a given point in space, is zero [27–47, 50]. Recently, the possibility of obtaining unipolar pulses, for which the electric area differs from zero, has become attractive [52, 53]. These pulses are capable of unidirectionally acting on charged particles and, consequently, to efficiently transfer momentum to charges, which makes it possible to use these pulses to accelerate charged particles, control the dynamics of wave packets, etc. [52].

The appearance in a resonant medium of light-induced gratings of the population difference and polarization in the case of coherent interactions of long not overlapping pulses with the medium was considered in [54–57]. The possibility of creating of such light-induced polarization and inversion structures in a resonant medium upon coherent propagation of single-cycle bipolar extremely short pulses and unipolar subcycle pulses under conditions that pulses do not overlap each other in the medium was studied in [46–50]. Collisions of self-induced transparency bipolar solitons were studied in [58–60] for the case of long pulses and in [42–45] for the case of extremely short pulses. Collisions of two unipolar subcycle pulses propagating in a medium that consists of a mixture of gaining and absorbing particles were considered in [31]. In [51], the dynamics of light-induced polarization and inversion structures was analyzed under conditions that subcycle pulses interact at the center of the medium. In [61], the collisional dynamics of two unipolar subcycle pulses was examined under consideration of soliton propagation through the medium in the medium. The authors of [66] investigated the properties of strongly coupled long-lived states of a system “electromagnetic field + matter,” which arise upon collisions of coherent pulses in a dense resonant medium (“polariton clusters”). It was shown that polariton clusters possess necessary properties to be base elements of all optical signal processing.

In this paper, we study situations in which unipolar subcycle pulses intersect and collide with bipolar single-cycle attosecond pulses in a medium, as well as situations in which, contrastingly to previous works, more than two pulses participate in the collision. We analyze the behavior of light-induced structures created by sequences of these pulses in the medium at different concentrations of absorbing particles. The influence of the radiation of traveling polarization waves on the dynamics of propagating pulses is considered. It is shown that, when extremely short pulses are overlapped in a medium, the state of a part of the medium on one side of the overlap region may differ

from the state of the region of the medium that is located on the other side of the region in which the pulses overlap with each other. In particular, we show that, in the regions located on opposite sides of the pulse overlap region, polarization waves with different spatial characteristics may form. These waves can propagate in opposite directions, and, if three pulses collide in the medium, the waves have different spatial frequencies.

In this paper, we consider the case in which the pulse duration is comparable with the period of the light wave, and the dimensions of the overlap region of the pulses are also on the order of the wavelength of the light wave. It is evident that, in this case, the incident fields cannot interfere with each other even with a short-term formation of a standing wave. Therefore, the dimensions of the zone that separates the parts of the medium with different properties is extremely small. This constitutes the fundamental difference between the case considered below and the situation in which multicycle bipolar femtosecond and longer pulses overlap with each other in the medium. In the latter case, the dimensions of the overlap region are equal to several tens, hundreds, or more wavelengths, and gratings are created as a result of the interference between overlapping beams [62].

THE THEORETICAL MODEL AND THE SYSTEM UNDER CONSIDERATION

To study collisions of unipolar subcycle and single-cycle attosecond pulses in a resonant medium, the system of Maxwell–Bloch equations was applied. Because the duration of exciting pulses is short, the system does not use either the approximation of slowly varying amplitudes or the rotating-wave approximation. As in [27–51], the medium was described in the two-level approximation using the density-matrix formalism. Calculations show that, if a greater number of levels of a medium are taken into account, the main features of the coherent propagation of pulses in two-level media still remain [32–34, 36, 50]; therefore, for simplicity, we will use the two-level approximation in this paper. The inhomogeneous broadening will be also neglected. The field is assumed to be linearly polarized, which reduces the problem to a scalar one. We also neglect the diffraction of radiation, which is justified for propagation lengths of beams that are smaller than the diffraction length.

Therefore, the examined systems of equations has the form

$$\begin{aligned} \frac{\partial \rho_{12}(z, t)}{\partial t} = & -\frac{\rho_{12}(z, t)}{T_2} + i\omega_0 \rho_{12}(z, t) \\ & - \frac{i}{\hbar} d_{12} E(z, t) n(z, t), \end{aligned} \quad (1)$$

$$\frac{\partial n(z,t)}{\partial t} = -\frac{n(z,t) - n_0(z)}{T_1} \quad (2)$$

$$+ \frac{4}{\hbar} d_{12} E(z,t) \text{Im} \rho_{12}(z,t),$$

$$P(z,t) = 2N_0 d_{12} \text{Re}(\rho_{12}), \quad (3)$$

$$\frac{\partial^2 E(z,t)}{\partial z^2} - \frac{1}{c^2} \frac{\partial^2 E(z,t)}{\partial t^2} = \frac{4\pi}{c^2} \frac{\partial^2 P(z,t)}{\partial t^2}. \quad (4)$$

Systems (1)–(4) contain the following parameters: P is the polarization of the medium, N_0 is the concentration of active centers, E is the electric-field strength, c is the speed of light in a vacuum, \hbar is the reduced Planck constant, ω_0 is the frequency of the resonant transition of the medium ($\lambda_0 = 2\pi c/\omega_0$ is the wavelength of the resonant transition), d_{12} is the dipole moment of the working transition, and n_0 is the difference between the populations of the two working levels in the absence of an electric field ($n_0 = 1$ for the absorbing medium).

Equations (1) and (2) describe the evolution of the off-diagonal element of the density matrix, ρ_{12} , and the difference $n \equiv \rho_{11} - \rho_{22}$ between the diagonal elements of the density matrix, which has the meaning of the population difference (inversion) between the ground and excited states of the two-level system. The off-diagonal element of the density matrix, ρ_{12} , is related to the polarization of the medium by formula (3), this polarization serves as a source of the field in wave equation (4).

System of Maxwell–Bloch equations (1)–(4) is actively used in the literature to study the coherent propagation of extremely short pulses in a resonant media [27–51]. Here, to analyze the collisional dynamics, system (1)–(4) was solved numerically. Bloch equations (1) and (2) for the density matrix were solved by the fourth-order Runge–Kutta method. Wave equation (4) was solved by the method of finite differences.

The spatial region of integration had a length of $L = 12\lambda_0$. The resonant medium was located along the z axis at the center of the region between the points $z_1 = 4\lambda_0$ and $z_2 = 8\lambda_0$. Exciting pulses also propagated along the z axis (Fig. 1). As previously in [47–51], to create a sequence of exciting pulses for the numerical calculation, zero boundary conditions were taken for the values of the field for the limits of the integration region, which corresponds to an ideal reflection of the radiation at the boundaries.

COLLISION OF A BIPOLAR SINGLE-CYCLE PULSE WITH A UNIPOLAR SUBCYCLE PULSE IN A MEDIUM

Extremely short pulses were sent to a medium from the left and from the right (see Fig. 1). An extremely

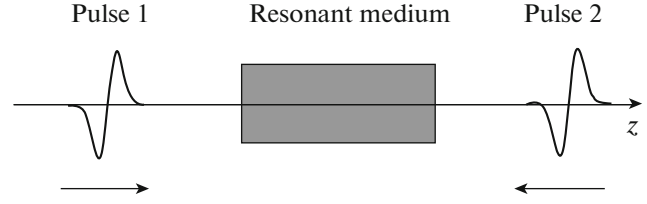


Fig. 1. Geometry of an examined system.

short pulse of a Gaussian shape was sent to the medium from the left (at the entrance to the medium):

$$E_1(t) = E_{01} \exp\left(-\frac{[t - \tau_1]^2}{\tau_{1p}^2}\right) \sin(\omega_0[t - \tau_1]). \quad (5)$$

From the right to the left, a unipolar subcycle pulse was sent, which also has a Gaussian shape,

$$E_2(t) = E_{02} \exp\left(-\frac{[t - \tau_2]^2}{\tau_{2p}^2}\right). \quad (6)$$

Here, $\tau_{1,2}$ are the time delays.

The parameters of the calculation are presented in Table 1.

The amplitudes of the exciting pulses were chosen such that the pulses would equalize the populations of the upper and lower levels; i.e., after the action of the pulses, the inversion $n = 0$ would be achieved.

The calculation results revealed the following dynamics of the system. Figure 2 illustrates the dynamics of inversion n , while Fig. 3 shows the dynamics of polarization P of the medium. Prior to their collision, the pulses transferred the medium to a state with a zero inversion (Fig. 2) and induced counterpropagating polarization waves (Fig. 3). Then, the pulses collided at the center of the medium at the point $z/\lambda_0 = 2$ at time moment $t \approx 0.015$ ps. Finally, these pulses continued to propagate and began to interact

Table 1. Parameters that were used in numerical calculations

Wavelength of resonant transition	$\lambda_0 = 700$ nm
Transition dipole moment	$d_{12} = 20$ D
Relaxation time of inversion	$T_1 = 1$ ns
Relaxation time of polarization	$T_2 = 1$ ps
Concentration of atoms	$N_0 = 5 \times 10^{14}$ cm ⁻³
Amplitude of field 1	$E_{01} = 9.55 \times 10^4$ esu units
Duration of pulse 1	$\tau_{1p} = 388$ as
Amplitude of field 2	$E_{02} = E_{01}$
Duration of pulse 2	$\tau_{1p} = \tau_{2p}$
Parameter of delay	$\tau_1 = \tau_2 = 2.5\tau_{1p}$

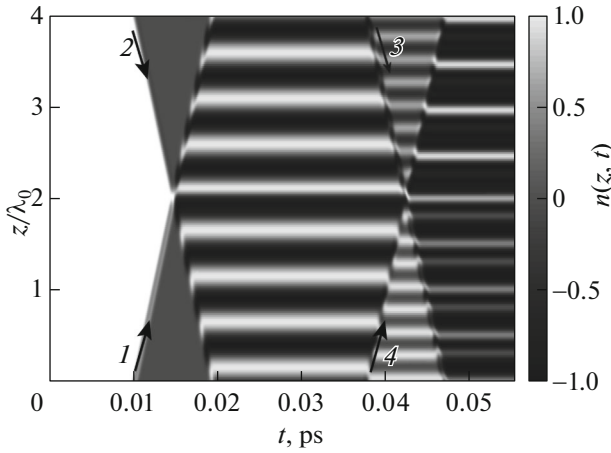


Fig. 2. Dynamics of population difference $n(z, t)$ under the action of bipolar single-cycle pulse 1 and unipolar subcycle pulse 2 colliding at the center of a medium (at the point $z/\lambda_0 = 2$) at time moment $t \approx 0.015$ ps. Calculation parameters are given in Table 1.

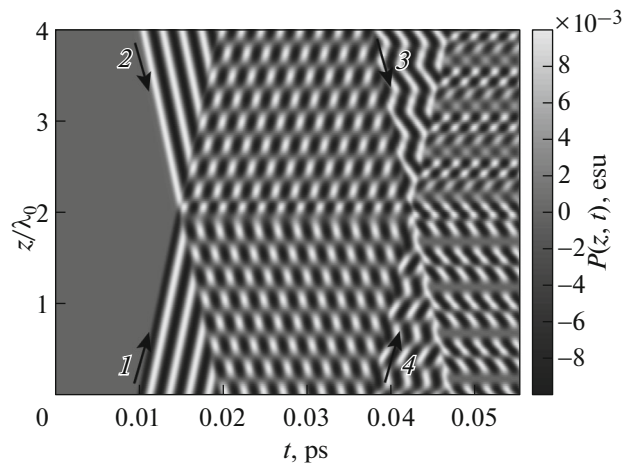


Fig. 3. Dynamics of polarization $P(z, t)$ under the action of bipolar single-cycle pulse 1 and unipolar subcycle pulse 2 colliding at the center of a medium (at the point $z/\lambda_0 = 2$) at time moment $t \approx 0.015$ ps. Calculation parameters are given in Table 1.

with polarization waves that run towards them and that were induced a moment before by the preceding pulses. As a result, in both halves of the medium, to the right and to the left of the point at $z/\lambda_0 = 2$, gratings of the population difference with a period of $\lambda_0/2$ (Fig. 2) and polarization waves appeared (Fig. 3). After that, the pulses came out of the medium, were “reflected” from the boundaries of the integration region and were sent again to the medium. They entered the medium at the time $t = 0.04$ ps. In Figs. 2 and 3, the moments of entrance of pulses are indicated by the arrows with numbers 3 and 4. At the time moment $t \approx 0.045$ ps, the pulses overlap with each other in the medium. Prior to this time moment, the pulses induced polarization waves in different parts of the medium, which traveled in opposite directions. This is clearly seen in Fig. 3 in the form of a characteristic zigzag structure on the left and on the right of the point at $z/\lambda_0 = 2$.

These polarization structures, running in opposite directions in different parts of the medium, vanished as soon as pulses overlapped each other at the point $z/\lambda_0 = 2$ at $t \approx 0.045$ ps. After the overlap of the pulses in the medium, quasi-harmonic gratings of the population difference appeared in the medium on the left and on the right of the point of collision $z/\lambda_0 = 2$ of the pulses, as well as more complex structures of polarization waves. Figure 4 shows these gratings after the emergence of the pulses from the medium at the time moment $t = 0.056$ ps.

Therefore, the dynamics of light-induced structures upon collision of a subcycle unipolar pulse with a single-cycle bipolar pulse is similar to the dynamics of light-induced structures that arise upon collisions of subcycle pulses [51] and upon propagation of

extremely short pulses that do not overlap in the medium [46–50]. The only exception is the above-mentioned interesting fact about the appearance of regions in the medium in which polarization waves that travel in opposite directions exist. This fact was not mentioned in previous studies [46–50].

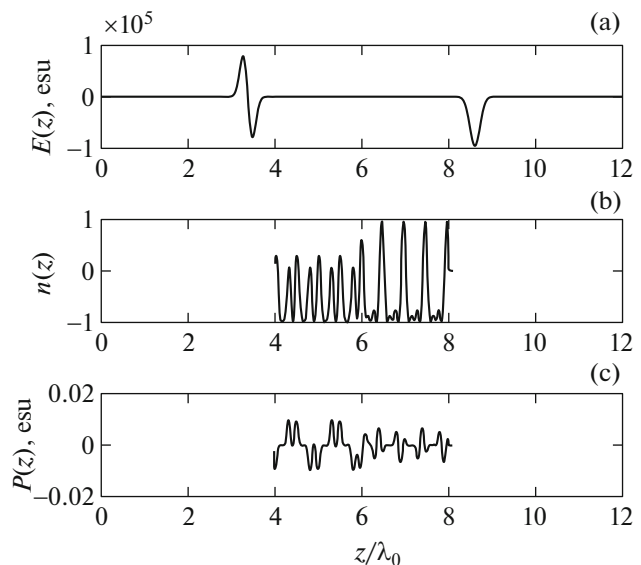


Fig. 4. (a) Excitation pulses emerged from a medium. Distributions of (b) population difference $n(z, t)$ and (c) polarization $P(z, t)$ after the exit of the pulses from the medium for the situations of Figs. 2 and 3 at moment of time $t = 0.056$ ps. The medium is located between the points at $z = 4\lambda_0$ and $z = 8\lambda_0$.

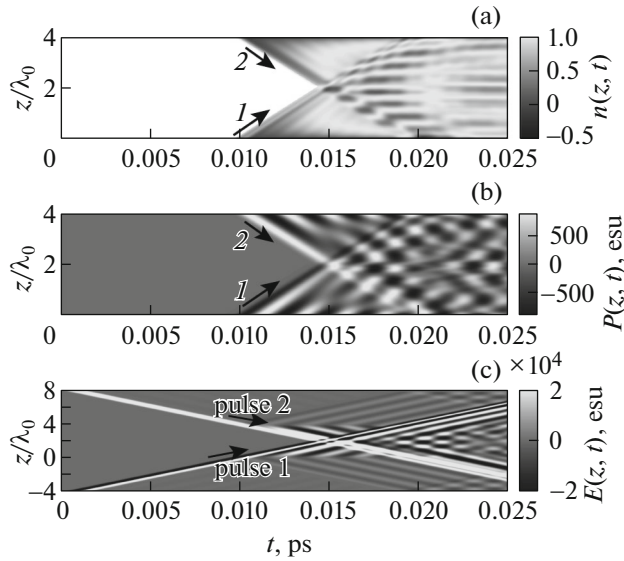


Fig. 5. Distributions of (a) population difference $n(z, t)$, (b) polarization $P(z, t)$, and (c) field. The medium in (c) is located between the points at $z = 0$ and $z = 4\lambda_0$.

THE INFLUENCE OF THE RADIATION OF POLARIZATION WAVES ON THE SHAPE OF PASSING PULSES

In the preceding example, as well as in [46–51], the concentration of atoms was so small that the excitation pulses remained almost unchanged during their propagation. However, generally speaking, induced traveling polarization waves may emit light after the transmitted pulse. Such a possibility was mentioned in [50], however, because the concentration of absorbing atoms is low, the magnitude of the emitted field is negligibly small and pulses propagating in the medium hardly change their shape. It is interesting to consider the case when the medium is optically dense. In the following example, the particle concentration was taken to be $N_0 = 5 \times 10^{19} \text{ cm}^{-3}$. The remaining parameters remained the same as in Table 1.

The behaviors of the inversion, the polarization, and the field are presented in Figs. 5a–5c, respectively. Pulses enter the medium at time moment $t = 0.01$ ps and immediately begin to change their shape upon propagation. Polarization waves created by pulses (Fig. 5b) emit light after the transmitted impulses, and it begins to affect the shape of the transmitted pulses. This leads to spreading of pulses as they propagate. In this case, the amplitude of the pulses decreases during their propagation; therefore, the inversion does not change significantly (Fig. 5a) and harmonic gratings are not formed. In the medium, a complex energy exchange between the field and the medium is observed. The spatial distribution of the field and the distribution of the polarization and the

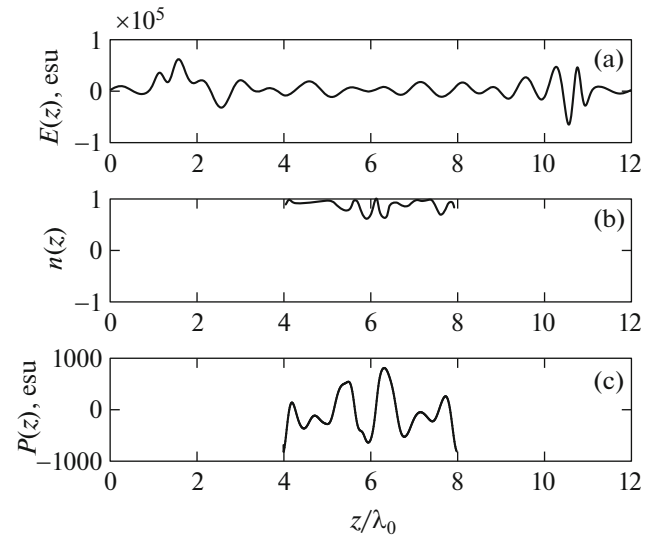


Fig. 6. Distributions of (a) the field, (b) population difference $n(z, t)$, and (c) polarization $P(z, t)$ for the situation of Fig. 5 at moment of time $t = 0.025$ ps. The medium is located between the points at $z = 4\lambda_0$ and $z = 8\lambda_0$.

inversion of the medium at the time moment $t = 0.025$ ps are shown in Fig. 6.

Interestingly, this effect of spreading of extremely short unipolar subcycle pulses is similar to the effect of formation of so-called “zero-area pulses” (0π pulses) [63, 64]. It is well known that, when a pulse with small area Θ , which is smaller than π , and with a short duration, which is shorter than relaxation times T_1 and T_2 , propagates in a resonant medium, a zero-area pulse (0π pulse) is formed. This effect has been known for a long time for the case of long pulses, in which case the notion of the pulse area is applicable [63, 64]. If a pulse with the initial area $\Theta < \pi$ propagates through a medium, then, in accordance with the McCall–Hahn area theorem, its area will tend to zero while the pulse propagates through the medium [9, 15, 16]. In this case, the envelope of the pulse becomes alternating-signed while propagating through the medium, and the area of the pulse tends to zero. This occurs because the energy absorbed at the leading edge of the pulse is reemitted by the medium back into the field, but in an antiphase. Such 0π pulses were predicted theoretically in [63] and were observed experimentally in the case of relatively long pulses [64]. A similar dynamics is observed in the case of bipolar extremely short single-cycle pulses, as was shown in [41].

COLLISION OF THREE UNIPOLAR SUBCYCLE PULSES IN A RESONANT MEDIUM

Let extremely short pulses be sent into a medium from the left and from the right (Fig. 1). The field that

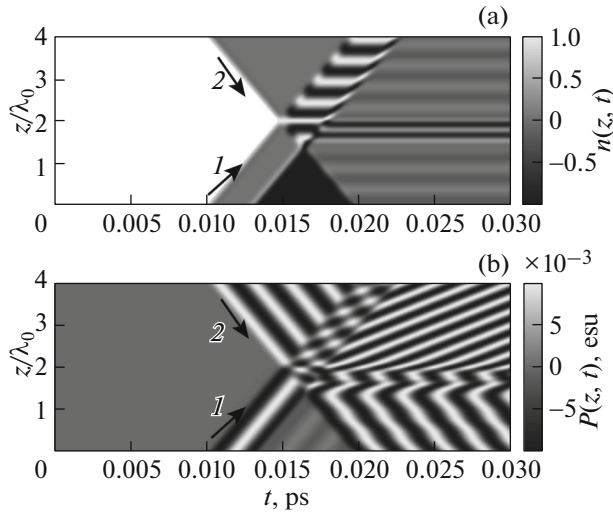


Fig. 7. Distributions of (a) population difference $n(z, t)$ and (b) polarization $P(z, t)$ upon excitation of a medium by a field of three unipolar subcycle pulses (7) and (8). The relaxation time is $T_2 = 5$ ps. The delay time is $\tau_4 = 10\tau_{1p}$. The remaining parameters are the same as in Table 1. The arrows indicate the propagation directions of the pulses. As in preceding examples, the pulses are overlapped approximately at the center of the medium (at the point $z/\lambda_0 = 2$) at the time moment $t \approx 0.015$ ps.

was sent from the left was taken as two subcycle unipolar pulses with some delay between them,

$$E_3(t) = -E_0 \exp\left(-\frac{|t - \tau_1|^2}{\tau_{1p}^2}\right) - 1.5E_0 \exp\left(-\frac{|t - \tau_3|^2}{\tau_{1p}^2}\right). \quad (7)$$

The field that was sent from the right also had a Gaussian profile of a unipolar subcycle pulse (as previously, the profile of the field on the left or the right boundary of the medium is meant),

$$E_4(t) = E_0 \exp\left(-\frac{|t - \tau_1|^2}{\tau_{1p}^2}\right). \quad (8)$$

The concentration of atoms absorbing pulses was taken to be small, as in the table, the relaxation time was $T_2 = 5$ ps, the amplitude of the field was $E_0 = 90000$ esu, and the delay was $\tau_3 = 10\tau_{1p}$. The remaining parameters were the same as in Table 1.

Figure 7 illustrates the dynamics of (a) the inversion and (b) the polarization in this case. In this example, the pulses are overlapped in the medium only once, and, as in the preceding examples, at the center of the medium (at the point $z/\lambda_0 = 2$) and at the time moment $t \approx 0.015$ ps, and they do not return to the

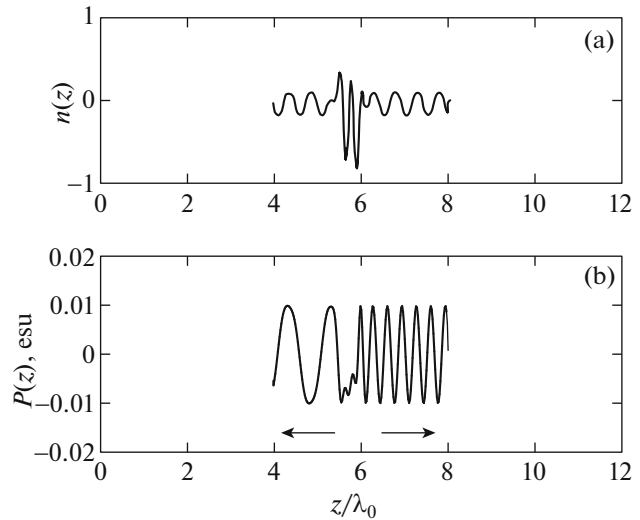


Fig. 8. Distributions of (a) population difference $n(z)$ and (b) polarization $P(z)$ at moment of time $t = 0.025$ ps after the exit of excitation pulses from the medium. The medium is located between the points at $z = 4\lambda_0$ and $z = 8\lambda_0$. The arrows in (b) show the directions of propagation of polarization waves.

medium no longer. As can be seen from Fig. 7a, after the overlapping of the pulses, a harmonic grating of the population inversion is formed in the right half of the medium. This example is interesting in so far as, as soon as the pulses leave the medium, harmonic polarization waves with different spatial frequencies are formed in its left and right halves (with periods λ_0 and $\lambda_0/3$, respectively; see Figs. 7 and 8b after the moment of overlap of the pulses at $t \approx 0.015$ ps). These polarization waves, which travel in opposite directions, are clearly seen in Fig. 8, which shows the instantaneous distributions of the (a) inversion and (b) polarization at the moment of time after the pulses left the medium. Correspondingly, the phase velocities of these waves are c and $c/3$.

Therefore, the example considered above illustrates the possibility of creating situations in which the state of a medium in its left half differs from its state in the right half. As can be seen from the preceding section, at large concentrations of atoms, the contribution of the radiation of traveling polarization waves becomes significant, which leads to a change in the shape of passed pulses. Correspondingly, it should be expected that, at high concentrations, the pattern shown in Figs. 7 and 8 will be blurred. This circumstance is confirmed and illustrated by Fig. 9. Excitation pulses will also spread, as is illustrated by Figs. 9c and 10, which show the distribution of the field in the medium in free space after the pulses left the medium.

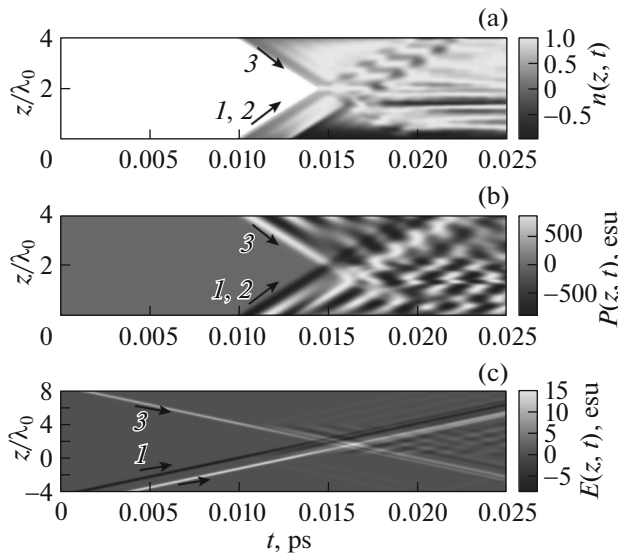


Fig. 9. The same as in Fig. 6 but at a larger concentration of atoms: $N_0 = 5 \times 10^{19} \text{ cm}^{-3}$. The remaining parameters are the same as in Fig. 6. The medium in (c) is located between the points at $z = 0$ and $z = 4\lambda_0$.

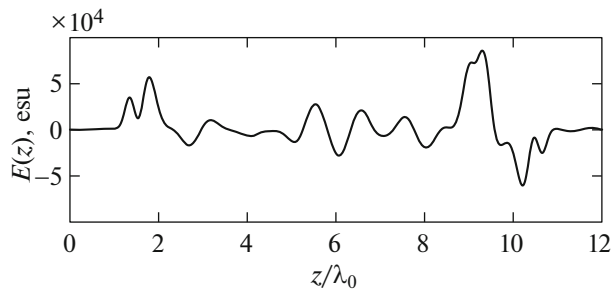


Fig. 10. Distribution of a field in space after the exit of colliding pulses from a medium at moment of time $t = 0.035 \text{ ps}$ for the situation shown in Fig. 8.

CONCLUSIONS

In this work, based on numerical modeling, we examined the dynamics of light-induced structures of polarization and inversion in a resonant medium upon propagation of overlapping bipolar single-cycle and unipolar subcycle attosecond pulses that coherently interact with the medium. We considered the cases of two overlapping pulses when the concentration of absorbing atoms is either small or comparatively large. In the first case, propagating pulses almost retain their shape, and the dynamics of light-induced structures of polarization and population inversion is similar to that previously studied by the authors of [46–51]. The considered polarization waves and the population-difference gratings can remain in the medium at times comparable to relaxation times. In the case of an optically dense medium, it becomes significant that polarization waves induced by the pulses become sources of

electromagnetic radiation that propagates after the passed pulses. This radiation is added to the field of the incident pulses and leads to the loss of subcyclicity and spreading.

Finally, we considered the case of three colliding video-pulses in a medium. In this case, as our calculations show, the state of the medium in its left half can differ from its state in the right half. For example, waves of polarization with threefold different spatial periods arise in them. These waves travel in opposite directions with significantly different phase velocities.

The considered examples show another possibility of ultrafast control of the medium state on the timescale of pulse duration. These circumstances can be used in ultrafast and nonlinear optics to create optical switches, laser-radiation deflectors, and short-term memory cells. Diffraction of light by similar structures can be used to measure relaxation time T_2 in different media, which was shown previously in the case of using long (nanosecond) pulses [55, 56].

To experimentally observe these effects, gases or quantum dots with long polarization relaxation time T_2 may be used. Quantum dots are a most suitable medium, since they have a discrete structure of levels, similarly to atoms, and they possess large transition dipole moments (dozens of Debyes). At low temperatures, polarization relaxation times T_2 can reach tens or hundreds of nanoseconds in them [65].

ACKNOWLEDGMENTS

This work was supported by a grant from the Russian Science Foundation, project no. 17-19-01097.

REFERENCES

1. F. Krausz and M. Ivanov, *Rev. Mod. Phys.* **81**, 163 (2009).
2. C. Manzoni et al., *Laser Photon. Rev.* **9**, 129 (2015).
3. F. Calegari et al., *J. Phys. B: At., Mol. Opt. Phys.* **49**, 062001 (2016).
4. L. Gallmann, C. Cirelli, and U. Keller, *Ann. Rev. Phys. Chem.* **63**, 447 (2012).
5. K. Ramasesha, S. R. Leone, and D. M. Neumark, *Ann. Rev. Phys. Chem.* **67**, 41 (2016).
6. M. F. Ciappina, J. A. Pérez-Hernández, and A. S. Landsman, *Rep. Prog. Phys.* **80**, 054401 (2017).
7. A. S. Landsman and U. Keller, *Phys. Rep.* **547**, 1 (2015).
8. M. Kozak, J. McNeur, K. J. Leedle, et al., *Nat. Commun.* **8**, 1 (2017).
9. S. L. McCall and E. L. Hahn, *Phys. Rev.* **183**, 457 (1969).
10. D. V. Skryabin and A. V. Gorbach, *Rev. Mod. Phys.* **82**, 1287 (2010).
11. J. M. Dudley, G. Genty, and S. Coen, *Rev. Mod. Phys.* **78**, 1135 (2006).
12. H. Leblond and D. Mihalache, *Phys. Rep.* **523**, 61 (2013).

13. D. U. Mihalache, *Roman. Rep. Phys.* **69**, 403 (2017).
14. P. G. Kryukov and V. S. Letokhov, *Sov. Phys. Usp.* **12**, 641 (1970).
15. I. A. Poluektov, Yu. M. Popov, and V. S. Roitberg, *Sov. Phys. Usp.* **18**, 673 (1975).
16. L. Allen and J. Eberly, *Optical Resonance and Two-Level Atoms* (Wiley, New York, 1975).
17. A. Zrenner et al., *Nature (London, U.K.)* **418**, 612 (2002).
18. T. H. Stievater, L. Xiaoqin, D. G. Stee, et al., *Phys. Rev. Lett.* **87**, 133603 (2001).
19. P. Borri, W. Langbein, S. Schneider, et al., *Phys. Rev. B* **66**, 081306 (2002).
20. M. Hosseini, B. M. Sparkes, G. Hétet, et al., *Nature (London, U.K.)* **461** (7261), 241 (2009).
21. M. Kolarczik et al., *Nat. Commun.* **4**, 1 (2013).
22. O. Karni, A. Capua, G. Eisenstein, et al., *Opt. Express* **21**, 26786 (2013).
23. A. Capua, O. Karni, G. Eisenstein, and J. P. Reithmaier, *Phys. Rev. B* **90**, 045305 (2014).
24. O. Karni, A. K. Mishra, G. Eisenstein, and J. P. Reithmaier, *Phys. Rev. B* **91**, 115304 (2015).
25. O. Karni, A. K. Mishra, G. Eisenstein, V. Ivanov, and J. P. Reithmaier, *Optica* **3**, 570 (2016).
26. I. A. Khanonkin, A. K. Mishra, O. Karni, et al., arXiv: 1708.06254 (2017).
27. V. P. Kalosha and J. Herrmann, *Phys. Rev. Lett.* **83**, 544 (1999).
28. J. Xiao, Z. Wang, and Z. Xu, *Phys. Rev. A* **65**, 031402 (2002).
29. X. Cai, J. Zhao, Z. Wang, and Q. Lin, *J. Phys. B: At., Mol. Opt. Phys.* **46**, 175602 (2013).
30. Y. Lin, I. H. Chen, and R. K. Lee, *Phys. Rev. A* **83**, 043828 (2011).
31. N. N. Rosanov, V. E. Semenov, and N. V. Vyssotina, *Laser Phys.* **17**, 1311 (2007).
32. N. V. Vyssotina, N. N. Rozanov, and V. E. Semenov, *JETP Lett.* **83**, 279 (2006).
33. N. N. Rosanov, V. E. Semenov, and N. V. Vyssotina, *Quantum Electron.* **38**, 137 (2008).
34. N. V. Vyssotina, N. N. Rozanov, and V. E. Semenov, *Opt. Spectrosc.* **106**, 713 (2009).
35. V. V. Kozlov, N. N. Rosanov, C. D. Angelis, and S. Wabnitz, *Phys. Rev. A* **84**, 023818 (2011).
36. N. N. Rozanov, *Dissipative Optical Solitons. From Micro- to Nano- and Atto- Scales* (Fizmatlit, Moscow, 2011), Chap. 17 [in Russian].
37. X. Song, W. Yang, Z. Zeng, R. Li, and Z. Xu, *Phys. Rev. A* **82**, 053821 (2010).
38. X. Song, Z. Hao, M. Yan, M. Wu, and W. Yang, *Laser Phys. Lett.* **12**, 105003 (2015).
39. S. Hughes, *Phys. Rev. Lett.* **81**, 3363 (1998).
40. A. V. Tarasishin, S. A. Magnitskii, and A. M. Zheltikov, *Opt. Commun.* **193**, 187 (2001).
41. A. V. Tarasishin, S. A. Magnitskii, V. A. Shuvaev, and A. M. Zheltikov, *Opt. Express* **8**, 452 (2001).
42. D. V. Novitsky, *Phys. Rev. A* **84**, 013817 (2011).
43. D. V. Novitsky, *Phys. Rev. A* **85**, 043813 (2012).
44. D. V. Novitsky, *J. Phys. B: At., Mol. Opt. Phys.* **47**, 095401 (2014).
45. D. V. Novitsky, *Opt. Commun.* **358**, 202 (2016).
46. R. M. Arkhipov, M. V. Arkhipov, I. V. Babushkin, and N. N. Rosanov, *Opt. Spectrosc.* **121**, 758 (2016).
47. R. M. Arkhipov, M. V. Arkhipov, I. V. Babushkin, A. Demircan, U. Morgner, and N. N. Rosanov, *Opt. Lett.* **41**, 4983 (2016).
48. R. M. Arkhipov, M. V. Arkhipov, I. V. Babushkin, A. V. Pakhomov, and N. N. Rosanov, *Quantum Electron.* **47**, 589 (2017).
49. R. M. Arkhipov, M. V. Arkhipov, A. V. Pakhomov, I. Babushkin, and N. N. Rosanov, *Laser Phys. Lett.* **14** (9), 1 (2017).
50. R. M. Arkhipov, A. V. Pakhomov, M. V. Arkhipov, I. Babushkin, A. Demircan, U. Morgner, and N. N. Rosanov, *Sci. Rep.* **7**, 12467 (2017).
51. R. M. Arkhipov, M. V. Arkhipov, A. V. Pakhomov, I. Babushkin, and N. N. Rosanov, *Opt. Spectrosc.* **123**, 610 (2017).
52. R. M. Arkhipov, A. V. Pakhomov, M. V. Arkhipov, I. Babushkin, Yu. A. Tolmachev, and N. N. Rozanov, *JETP Lett.* **105**, 408 (2017).
53. R. M. Arkhipov, A. V. Pakhomov, M. V. Arkhipov, I. Babushkin, Yu. A. Tolmachev, and N. N. Rosanov, *Laser Phys.* **27**, 053001 (2017).
54. I. D. Abella, N. A. Kurnit, and S. R. Hartmann, *Phys. Rev.* **141**, 391 (1966).
55. E. I. Shtyrkov, V. S. Lobkov, and N. G. Yarmukhamev, *JETP Lett.* **27**, 648 (1978).
56. S. A. Moiseev and E. I. Shtyrkov, *Sov. J. Quantum Electron.* **21**, 403 (1991).
57. E. I. Shtyrkov, *Opt. Spectrosc.* **114**, 96 (2013).
58. M. J. Shaw and B. W. Shore, *J. Opt. Soc. Am. B* **8**, 1127 (1990).
59. A. A. Afanas'ev, V. M. Volkov, V. V. Dritz, and B. A. Samson, *J. Mod. Opt.* **37**, 165 (1990).
60. V. V. Kocharovski, V. V. Kocharovski, and E. R. Golubyatnikova, *Comput. Math. Appl.* **34**, 773 (1997).
61. E. M. Belenov, A. V. Nazarkin, and V. A. Ushchapovskii, *Sov. Phys. JETP* **73**, 422 (1991).
62. H. J. Eichler, E. Günter, and D. W. Pohl, *Laser-Induced Dynamic Gratings* (Springer, Berlin, New York, Heidelberg, Tokyo, 1981).
63. M. D. Crisp, *Phys. Rev. A* **1**, 1604 (1970).
64. J. E. Rothenberg, D. Grischkowsky, and A. C. Balant, *Phys. Rev. Lett.* **53**, 552 (1984).
65. M. Bayer and A. Forchel, *Phys. Rev. B* **65**, 041308 (2002).
66. S. N. Bagaev, V. S. Egorov, V. G. Nikolaev, I. A. Chechotin, and M. A. Chekhonin, *Russ. J. Phys. Chem. B* **9**, 582 (2015).